

DEEP LEARNING-BASED POLARIMETRIC SAR AND OPTICAL IMAGE FUSION TO MAP OIL PALM ALONG RIVERS

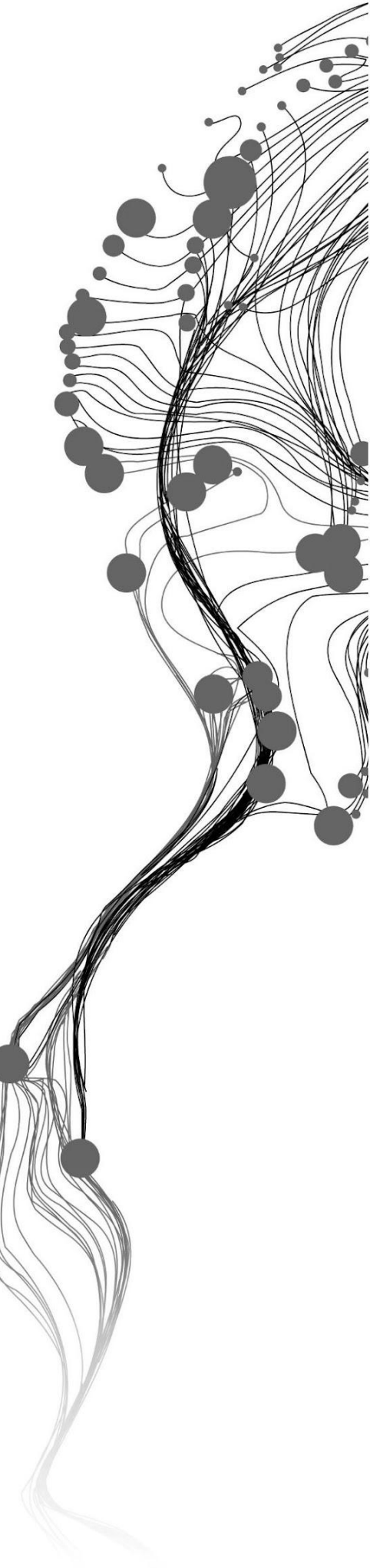
MUHAMMAD AFIF FAUZAN

June, 2023

SUPERVISORS:

Dr. I. C. van Duren

Dr. R. Vargas Maretto



DEEP LEARNING-BASED POLARIMETRIC SAR AND OPTICAL IMAGE FUSION TO MAP OIL PALM ALONG RIVERS

MUHAMMAD AFIF FAUZAN

June, 2023

Thesis submitted to the Faculty of Geo-Information Science and Earth Observation of the University of Twente in partial fulfilment of the requirements for the degree of Master of Science in Geo-information Science and Earth Observation.
Specialization: Geo-information Science and Earth Observation for Environmental Modelling and Management

SUPERVISORS:

Dr. I. C. van Duren

Dr. R. Vargas Maretto

THESIS ASSESSMENT BOARD:

Dr. T. Wang (Chair)

Leila Maria Garcia Fonsesca (External Examiner, The National Institute of Space Research - INPE Brazil)

DISCLAIMER

This document describes work undertaken as part of a programme of study at the Faculty of Geo-Information Science and Earth Observation of the University of Twente. All views and opinions expressed therein remain the sole responsibility of the author, and do not necessarily represent those of the Faculty.

ABSTRACT

The cultivation of vegetable oil crops such as oil palm often occurs illegally in ecologically significant areas such as river banks despite being protected by law. More lands including river banks are expected to be converted into oil palm plantations to meet the growing demand for palm oil, but the magnitude of this problem is currently undocumented. In this study, a complex-valued deep learning classification model to combine complex-valued Synthetic Aperture Radar (SAR) and optical images was developed for mapping oil palm plantations. The proposed model was compared with several baseline classification models. The result suggested that the complex-valued neural network trained with complex-valued Sentinel-1 SAR alone achieved the highest accuracy with an F1-score of 0.972. This model was applied to classify multi-temporal SAR images from 2017 to 2021 to produce multi-temporal oil palm plantation distribution maps on the riparian zones. It was found that oil palm cultivation on river banks increased with an average rate of nearly 4% per year. By 2021, the total oil palm plantation areas on river banks reached 8500 Ha which accounted for 29% of river banks in the study area. However, as the model failed to detect sparse and open-canopy oil palm plantations, the result should be interpreted carefully as solely productive oil palm plantation areas indicated by their closed-canopy characteristic once the trees reach a mature age and start producing palm fruit bunch.

ACKNOWLEDGEMENTS

I would like to thank my supervisors, Iris and Raian, for their support and expertise. The insight, guidance, feedback, and patience they provided have been essential in writing this thesis. I am thankful for the opportunity to work under their supervision.

I would also like to thank the GEM programme management team for arranging this joint-programme. I am thankful for the opportunities for intellectual growth and the exposure to diverse perspectives. Participating in the GEM programme has been a wonderful experience.

Lastly, I would like to acknowledge my family, friends, and colleagues for their encouragement and understanding. Thank you for believing in me and for being a part of this incredible journey.

TABLE OF CONTENTS

1. INTRODUCTION	1
1.1. Context of palm oil production	1
1.2. Remote sensing for oil palm plantation mapping	2
1.3. Deep learning for Earth observation	4
1.4. The Potential of multi-modal fusion techniques	5
1.5. Problem statement	6
1.6. Objectives, research questions, and intended outputs	6
2. STUDY AREA AND DATASETS	7
2.1. Study Area	7
2.2. Datasets and Preprocessing	7
2.3. Computing Infrastructure and Software	10
3. METHODS	11
3.1. Training data preparation	11
3.2. Classification model development	12
3.3. Multi-year mapping of oil palm on river banks	15
4. RESULTS	16
4.1. Deep learning classification model outputs	16
4.2. Oil palm plantations on the riparian zone	16
5. DISCUSSION	19
6. CONCLUSION AND RECOMMENDATION	22
6.1. Conclusion	22
6.2. Recommendation	22

1. INTRODUCTION

1.1. Context of palm oil production

The past two decades have witnessed a rise in global demand for vegetable oil (OECD/FAO 2021). Among vegetable oil crops (i.e. soybean, sunflower, rapeseed), oil palm (*Elaeis guineensis*) which produces palm fruit bunch as a source of palm oil is considered the most efficient crop yielding over six times more oil on the same land area (Sheil et al. 2009). It is highly productive as the fruit is harvestable every ten days once the tree reaches the mature age of three years and will be productive until it peaks at the age of 25 years (Murphy et al. 2021). A high preference for palm oil due to its lower price compared to other vegetable oil sources is apparent as its derivatives can be found in a wide range of products, including cooking oil, food, cleaning products, and cosmetics (Meijaard et al. 2018). Recent policies have also promoted the increased use of palm oil for biodiesel as an alternative to fossil fuel (Silalahi et al. 2020). This appeal has triggered a rapid expansion of oil palm, with most plantations can be found in the Southeast Asia region (Koh & Wilcove 2008).

In 2008 Indonesia surpassed Malaysia in palm oil production and has since become the leading palm oil producer, contributing to half of the global palm oil production share. More than half of the total produced palm oil is used for export (Shigetomi et al. 2020). According to official statistics, the area of oil palm plantations in Indonesia was 14.60 million hectares in 2019, with dominant distribution in the Sumatera and Kalimantan regions (BPS-Statistics Indonesia 2019). Most of the plantations are managed by large corporations, while around 40% of plantation areas are cultivated by smallholder farmers (Jelsma et al. 2017).

Indonesian regulations classify producers based on the size of their plantations. Smallholder farmers who independently cultivate oil palm on land of fewer than 25 hectares are exempted from more complex requirements for obtaining permits as compared to large-scale plantations by companies (Paoli et al. 2013). Additionally, there is the nucleus-plasma scheme, where large-scale plantation companies are mandated to allocate 20% of the managed land to smallholder farmers (McCarthy et al. 2012) even though only 22% of oil palm plantation companies comply with this obligation so far (Darto 2023). With plantation maintenance and production being labor intensive for all-year-round harvest, the palm oil sector creates jobs and provides stable income, contributing to poverty alleviation and stimulating rural development (Budidarsono et al. 2013).

Despite the benefits, palm oil production is often associated with environmental problems (Koh & Ghazoul 2008). The establishment of monoculture oil palm plantations often takes place in ecologically significant areas (Abood et al. 2015), such as river banks, which serve as crucial transitional habitats between freshwater and terrestrial ecosystems (Sheaves et al. 2018). River banks are often naturally covered by vegetation playing vital roles in flood and erosion control (Decamps et al. 2009, Horton et al. 2018), while also serving as a habitat and movement corridor for terrestrial biodiversity (Gray et al. 2019). Their role in maintaining water quality is important for aquatic biodiversity as well as for communities downstream relying on rivers as their source of water and food from capture fisheries (Giam et al. 2015). The establishment of oil palm on river banks has been reported to degrade water quality (Carlson et al. 2014) and reduce species of birds (Mitchell et al. 2018), amphibia (Paoletti et al. 2018), fishes (Giam et al. 2015), and other invertebrates (Mercer et al. 2014). Conversely, maintaining riparian buffers close to the plantation could conserve bird species (Mitchell et al. 2018) which in turn would be natural pest control from common insect pests and reduce the need for pesticides (Koh et al. 2008).

Due to their importance, riparian buffers are protected by law although the width criteria vary across regions (Luke et al. 2019). In Indonesia, the law to protect areas up to 100 meters on each river bank can be traced to the year 1991 (Government Regulation 35/1991). This criterion is further adopted in derivatives regulations including the Spatial Planning Act which obliges local governments to allocate these protected areas in their zoning regulation of spatial plans (Law of the Republic of Indonesia 26/2007). Nevertheless, oil palm cultivation continues to expand on river banks, particularly by smallholder producers who are likely to operate illegally without licenses and less strictly monitored by authorities (Bakhtary et al. 2021, Sheaves et al. 2018).

In addition to legislative efforts to protect riparian zones, the growing consensus from consumers to opt for sustainably-produced palm oil has ignited schemes to ensure sustainable practices in the supply chain through product certification (Ivancic & Koh 2016). Sustainable certifications such as Roundtable Sustainable Palm Oil (RSPO) require producers to comply with local regulations and categorize river banks as high conservation value areas to be protected according to High Conservation Value (HCV) standard (Lucey et al. 2018). While RSPO certification is voluntary, the Indonesian Sustainable Palm Oil (ISPO), introduced by the Indonesian government in 2011 is compulsory and requires all oil palm growers to certify their plantations by 2025 (Presidential Regulation of the Republic of Indonesia Number 44/2020). However, both regulatory measures and product certification are yet to show effectiveness. The implementation of the former has been inadequate due to poor enforcement by the authorities (Rukmana 2015), while the latter has been slowly adopted by producers particularly smallholders who face barriers such as a lack of land legality registration documents and associated costs (Hidayat et al. 2015). With more lands including river banks expected to be converted into oil palm plantations to fulfill the growing demand for vegetable oil (Corley 2009), obtaining accurate information on the distribution of oil palm on river banks is needed to determine proper measures for improved land management and sustainable palm oil production.

1.2. Remote sensing for oil palm plantation mapping

Remotely sensed satellite images have been widely utilized in providing spatially explicit information on the earth's surface phenomena due to their effectiveness in capturing a wide area repetitively (Campbell & Wayne 2011), including oil palm mapping. Beyond oil palm plantation distribution, examples of oil palm traits that can be estimated from remote sensing images are stands age (Carolita et al. 2019, Chemura et al. 2015), aboveground biomass (Morel et al. 2012, Khasanah et al. 2015), and plantation establishment period using time-series analysis (Xu et al. 2020, Danylo et al. 2021). More applied studies have also used satellite images to assess the magnitude of natural forests and peatland conversion into oil palm plantations (Koh et al. 2011, Gaveau et al. 2022). These variables require oil palm plantation distribution to be mapped accurately first to ensure the estimated variable is associated with oil palm and not other land covers.

Various studies have utilized multispectral images produced from passive optical sensors due to data availability and interpretability to map oil palm distribution. Passive optical sensors record radiated electromagnetic energy from the visible to infrared spectrum from object on the earth's surface that reflects sunlight (Campbell & Wayne 2011). Vegetation objects including oil palms canopy highly reflect lights on green (495 - 570 nm) and near-infrared (700 - 1100 nm) wavelengths compared to other parts of the electromagnetic spectrum, in which chlorophyll content and internal tissue are responsible for the intensity of reflected energy on each spectral band (Campbell & Wayne 2011). Some of the popularly used multispectral images for mapping oil palm distribution in the oil palm hotspot region of Malaysia and Indonesian Sumatera and Kalimantan are MODIS (Koh et al. 2011, Miettinen et al. 2016, Xu et al. 2020) and Landsat (Gaveau et al. 2016, Lee et al. 2016, Miettinen et al. 2018, Shaharum et al. 2020). In the past few years, the Sentinel-2 satellite constellation has become the additional open data source option with a higher spatial resolution (Nomura et al. 2019). The main limitation of using images from passive optical sensors is the cloud coverage which is often present in the region where oil palm is grown (Pohl et al. 2016).

Compared to passive optical sensors, active sensors of Synthetic Aperture Radar (SAR) transmit their own energy on the microwave spectrum which is less affected by clouds and independent of sunlight presence (Campbell & Wayne 2011). Each pixel of produced SAR images represents the intensity of backscattered energy, which is affected by the shape, texture, and size of the recorded objects. The wavelength used by the SAR instrument affects the penetration and the size of the object it can interact with, such as the C-band (3.8 - 7.5 cm) that interacts with vegetation canopy while the L-band (15 - 30 cm) penetrates deeper and interact with branches (Pohl & van Genderen 2016). SAR instruments can transmit and receive electromagnetic wavelength in a certain travel direction also known as polarization. The polarization can be either horizontal transmission-horizontal reception (HH), horizontal transmission-vertical reception (HV), vertical transmission-vertical reception (VV), or vertical transmission-horizontal reception (VH). HH and VV are also known as co-polarization, while HV and VH are known as cross-polarization. Different polarizations help to reveal more detail on the earth's surface objects. Instruments such as PALSAR L-band and Radarsat-2 C-band are categorized as quad-polarimetric or full polarimetric due to their capability of transmitting and receiving signals in all polarizations. Sentinel-1 C-band SAR instrument, on the other hand, can only use two polarizations and hence is categorized as dual-polarimetric (Hajnsek & Desnos 2021). Aside from the cloud-penetrating ability, SAR images offer distinct backscattered signals that are influenced by the unique crown shape of oil palm trees, setting them apart from surrounding vegetation (Miettinen & Liew 2011). With these properties, SAR images have often been used in mapping oil palm distribution (Darmawan et al. 2020, Li et al. 2015, Cheng et al. 2016, Cheng et al. 2018). However, due to the similarity of crown shape from coconut trees, it should be used carefully in coastal areas where coconut tree cover often occurs (Gaveau et al. 2022, Descals et al. 2023). The limitation that is consistently found in several studies is the inability of SAR images to detect open-canopy oil palm plantations, which is likely to be found in young or newly established plantations (Koh et al. 2011, Descals et al. 2019, Descals et al. 2021).

Previously mentioned studies have only used backscatter intensities from different polarization images and neglected the valuable information contained in phase-preserved SAR data (Trisasonoko et al. 2022). This phase occurs in the complex signal domain and allows polarimetric SAR (PolSAR) analysis to characterize different scattering behavior from ground objects, which potential in land cover mapping is highlighted in recent studies (Li & Bijker 2019, Braun & Offermann 2022, Trisasonoko et al. 2022). Commonly available algorithms were not designed to handle complex values, thus a way to incorporate the benefits of polarimetric SAR into image analysis is by converting the complex-valued polarimetric representation of SAR images into real value representations (Gao et al. 2017, Zhu et al. 2021).

Besides diverse data sources, various methods have also been demonstrated to map oil palms from satellite images. Manual digitization through visual interpretation of moderate and high spatial resolution satellite images, although could be time-consuming over a large area, is still used (Miettinen et al. 2018, AURIGA 2019, Gaveau et al. 2022). Automating the task with supervised image classification becomes preferable consequently, where each pixel of an image is assigned to a specific target class by an algorithm trained with pixel samples for each target class to be mapped (Knudby 2021). Conventional per-pixel classification algorithms such as Mahalanobis Distance and Maximum Likelihood were popular due to the simplicity and availability in most image processing software and provide output maps with sufficient accuracy when a simple classification scheme is used (Cheng et al. 2016, Cheng et al. 2018). Additionally, more sophisticated computations offered by advanced classifiers such as Support Vector Machines and Random Forests were found to outperform conventional classification algorithms in oil palm mapping (Li et al. 2015, Nooni et al. 2016, Cheng et al. 2018). Some of the benefits of using these classifiers are the ability to perform well with small samples and more image features beyond native spectral bands (Pohl & van Genderen 2016). Spectral indices have been used to enrich the predictive variables in the classification (Nomura et al. 2019, Monsalve-Tellez et al. 2022). On top of that, attempts to integrate textural features to overcome the limitation of per-pixel classification approaches in considering neighborhood pixels

have been demonstrated in several studies (Cheng et al. 2018, Sarzynsky et al. 2020, Monsalve-Tellez et al. 2022) and proven helpful in discriminating oil palm plantations to typology level (Descals et al. 2019).

1.3. Deep learning for Earth observation

Successful implementations of artificial neural networks in the computer vision community have received much attention and motivated the rising adoption of the approach in earth observation remote sensing applications. Convolutional neural network (CNN) algorithms are commonly used as they employ convolutional layers that are designed to process gridded data of raster images. On a convolutional layer, a filter is applied over a kernel across the input images to extract the spatial and spectral features (Prince 2023). The arrangement of multiple convolutional filters mimics a network, enabling CNNs to learn hierarchical representations and iteratively update the weight of convolutional filters to fit the learned features to a certain target class under a supervised scheme (Ma et al. 2019). Examples of vision tasks that can be done with CNNs are scene classification, object detection, and semantic segmentation (Prince 2023). In the remote sensing community, semantic segmentation is also known as supervised pixel-wise image classification (Kemker et al. 2018) (Figure 1.1).

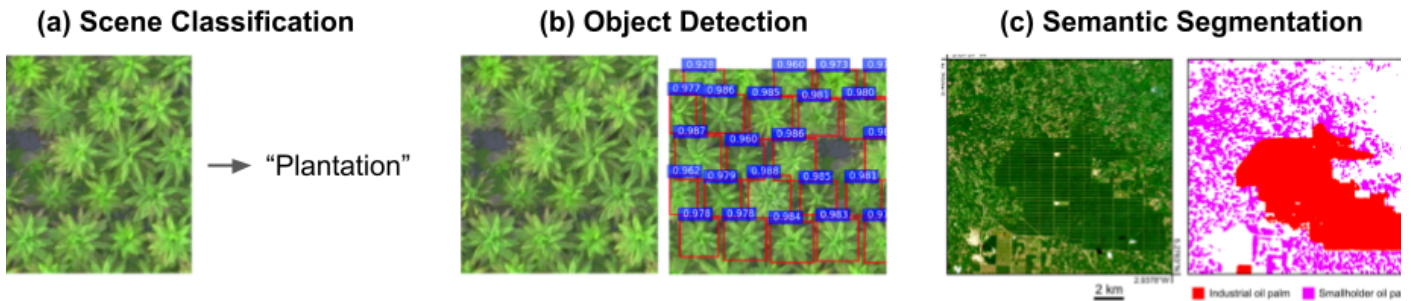


Figure 1.1. CNNs can be used to (a) classify a remote sensing image scene, (b) detect certain objects, and (c) classify land use to typology level e.g. industrial and smallholder plantation by learning spatial context (Liu et al. 2020, Descals et al. 2021).

With the operation nature to take into account neighborhood pixels in each kernel processing, performing pixel-wise image classification using CNN requires the network to be trained with polygons or area-based input rather than individual pixel values (Prince 2023). Therefore, the input to train the algorithms should consist of remotely sensed earth observation image subsets and their same-sized corresponding polygon or raster dataset with labeled pixels of target classes known as labeled datasets or reference maps. The extensive convolutional layers used in the algorithms, memory usage, and area-based input requirement separate the deep learning approaches from classic machine learning algorithms (Yuan et al. 2021).

As the structure of a CNN is modifiable, various deep learning architectures have been proposed for remote sensing image classification (Yuan et al. 2021). One of the most popular deep learning architectures is UNet, which is a CNN-based algorithm first proposed for supervised image segmentation in biomedical fields (Ronneberger et al. 2015). Its architecture consists of an encoder and a decoder. The encoder utilizes convolutional layers and max pooling operations to downsample input images and extract features. Meanwhile, the decoder employs deconvolution layers to upsample and reconstruct the dimension and classify the learned features to generate an output map. To retain spatial information from earlier layers with low-semantic features to later layers with high-semantic features, lateral connections are incorporated at corresponding levels of convolution and deconvolution layers. (Ronneberger et al. 2015). The final layer is a convolutional layer with a filter size of 1 x 1 and a sigmoid or softmax activation function that predicts and classifies the target class by assigning probabilities to each pixel in the feature map. (Figure 1.2).

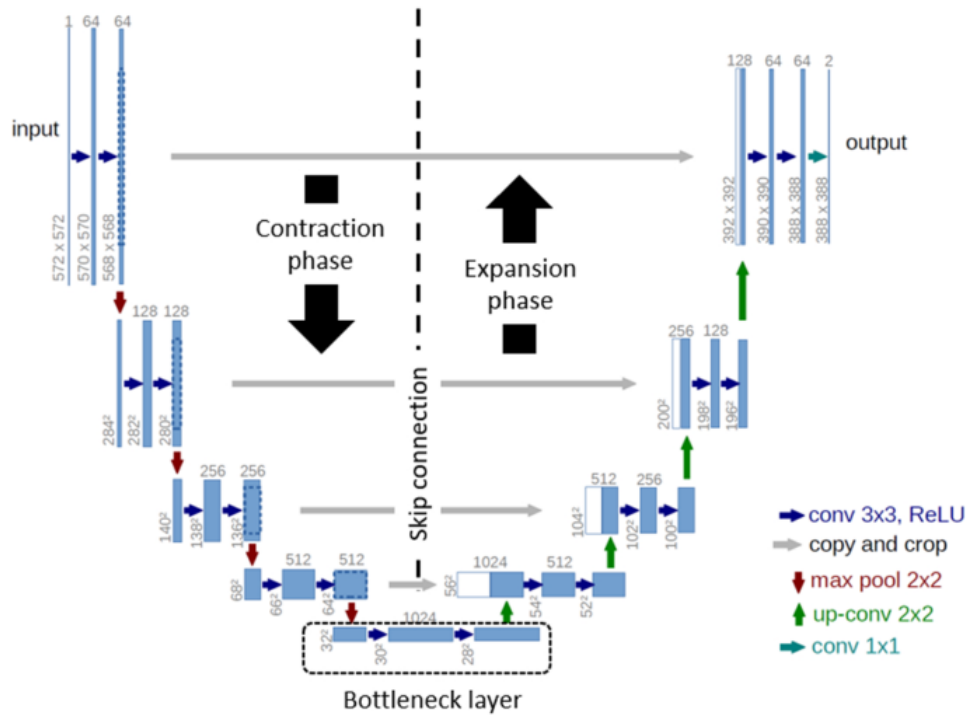


Figure 1.2. UNet architecture (Modified from Ronneberger et al. 2015)

UNet has shown robustness in differentiating forest cover and deforested areas (Maretto et al. 2021), mapping land cover (Solorzano et al. 2021), and coconut tree distribution (Descals et al. 2023). For oil palm mapping, Dong et al. (2019) applied a modified architecture of UNet to differentiate oil palm and other land covers from high spatial resolution images. Using different CNN architecture, Descals et al. (2021) exploited CNNs' ability in recognizing spatial context to improve further their previous study using a classic machine learning algorithm (Descals et al. 2019) in distinguishing between industrial and smallholder oil palm plantations based on the harvest-road spatial patterns on moderate spatial resolution images. Such a specific task is impossible to perform with traditional classifiers that only consider spectral information from individual pixels rather than the spatial context of input images.

For SAR data, the interest in exploiting phase data contained in the complex-valued SAR images has been growing. To accommodate the processing of complex-valued SAR images, recent studies have designed CNNs that is consisted of convolutional layers that are able to process complex-valued data (Mulissa et al. 2019, Barrachina et al. 2022a). These complex-valued CNNs were reported to outperform the equivalent real-valued CNNs in image classification.

1.4. The Potential of multi-modal fusion techniques

Remote sensing image fusion refers to the method of producing new images based on images from different properties, such as different acquisition periods, resolutions, or sensors. The objective of image fusion is to increase the interpretability of the image which could improve the accuracy of classification (Pohl et al. 2016). While a simple band stacking from different images is debatable to count as image fusion (Pohl & van Genderen 2016, Sebastianelli et al. 2021), such a simple approach has been demonstrated largely by combining images from optical and SAR sensors and benefited oil palm mapping (Torbick et al. 2016, Nomura et al. 2019, Descals et al. 2019, Sarzyński et al. 2020, Solorzano et al. 2021, Monsalve-Tellez et al. 2022, Zheng et al. 2022). The combination of multi-sensor images from different modalities is known as multimodal image fusion, driven by the open data policy of moderate optical and SAR images from earth observation missions (Torbick et al. 2016).

This previously mentioned approach of combining source images before feeding them to a classification algorithm is categorized as an early fusion paradigm where fusion occurred on the pixel level (Sebastianelli et al 2021). Contrary to this early fusion paradigm, fusion occurred at the feature level in the late fusion paradigm prior to being classified to produce an output map (Pohl & van Genderen 2016, Yuan et al. 2021). This configuration was made possible with the modifiable nature of neural networks. The late fusion approach was implied to provide better results than the early fusion mechanism (Hafner et al. 2022, Sebastianelli et al. 2021).

1.5. Problem statement

Oil palm plantations are expanding to river banks which are important for biodiversity conservation. These areas are protected by law and should not be used for oil palm plantations. However, violations are increasingly done particularly by smallholder producers. The magnitude of this problem is presently unreported, emphasizing the importance of oil palm mapping on river banks. With the demonstrated benefit of complex-valued PolSAR images as well as the fusion of SAR and optical images, a deep learning-based late fusion approach of complex-valued PolSAR and optical images has the potential to enhance the accuracy of oil palm mapping on river banks. However, the accuracy of this approach is currently unknown yet.

1.6. Objectives, research questions, and intended outputs

This study aims to design and test a late-fusion approach of complex-valued Sentinel-1 SAR images and Sentinel-2 optical images based on supervised deep learning to map oil palms on river banks. The specific objectives, research questions, and intended outputs are presented in Table 1.1.

Table 1.1. Specific objectives, research questions, and intended outputs

Specific objectives	Research questions	Intended outputs
Test the performance of deep learning-based late-fusion approach of complex-valued Sentinel-1 SAR images and Sentinel-2 optical images to map oil palm	How accurate is the oil palm map produced from deep learning classification model develop based on the fusion of complex-valued SAR and optical images?	<ul style="list-style-type: none"> ● Accuracy metrics of oil palm maps produced from deep learning classification model
Map and quantify the area of oil palm plantations on river banks annually over a five-year period	How large is the occupancy of oil palm on river banks over a five-year period?	<ul style="list-style-type: none"> ● Riparian oil palm distribution map ● Bar chart showing the area of oil palm plantations on river banks over a five-year period

2. STUDY AREA AND DATASETS

2.1. Study Area

Riau Province is located on Sumatra Island, Indonesia. Its area is known as the habitat of critically endangered elephants, tigers, and orangutans (Meijaard et al. 2018), continuously threatened by the extensification of oil palm cultivation. Being the largest palm oil-producing region in Indonesia, the oil palm cultivation area in Riau Province is reported to be 2.82 Mha with nearly half of the total cultivated area being smallholder-type plantations (BPS-Statistics Indonesia 2019). This study focuses on the northern region of Riau Province which includes Rokan Hulu and Rokan Hilir Regency (Figure 2.1). *Hulu* and *hilir* are Indonesian terms for upstream and downstream respectively, representing a gradient of elevation from highland in the southwest and lowland areas towards the northeast of the study area.



Figure 2.1. The study area covers Rokan Hulu and Rokan Hilir Regency in the northern part of Riau.

2.2. Datasets and Preprocessing

2.2.1. Sentinel-1 Synthetic Aperture Radar (SAR) images

Sentinel-1 images are open-access data provided by Sentinel-1 satellite mission operating in the C-band (5.5 cm wavelength). The sensor mainly records images over land in the Interferometric Wide (IW) swath mode in dual polarization for image acquisition where signals are polarized in vertical transmission-vertical reception (VV) and

vertical transmission-horizontal reception (VH) within 250 km swath width. The images are stored in SAR geometry where each pixel size is 2.3 x 14.1 m in range and azimuth direction respectively while representing complex values (real (i) + imaginary (q) components). Level-1 Single Look Complex (SLC) in IW mode covering the study site was obtained from the Copernicus Open Access Hub for the years 2017 to 2021. The phase-preserving SLC products were processed with the Sentinel Application Platform (SNAP) to derive dual polarimetric covariance matrix C2, which together with the coherency matrix are a common representation of complex-valued SAR stored in the off-diagonal elements of the matrix (Mullissa et al. 2019, Hansen et al. 2020). The diagonal elements of the matrix are real-valued, which represents the VV and VH polarization images. Figure 2.2 summarizes the steps to derive the C2 matrix.

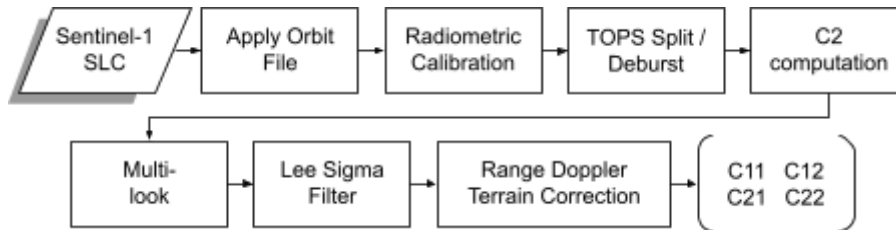


Figure 2.2. Workflow of Sentinel-1 SLC image preprocessing to derive dual-polarimetric covariance matrix. The diagonal elements of C11 and C22 represent the intensity of VV and VH respectively (σ°), while the off-diagonal elements represent complex values.

First, the precise orbit information was retrieved from the Copernicus Precise Orbit Determination (POD) and applied to the metadata of the Sentinel-1 SLC product to increase the geolocation accuracy. The data were radiometrically calibrated with complex output. As a consequence of the Terrain Observation with Progressive Scan (TOPS) IW acquisition mode, images are split and debursted to remove black borders between bursts prior to remerged. The dual polarimetric covariance matrix C2 was computed, which procedure is detailed by Mandal et al. (2019). A multi-look process and the Lee Sigma filter were applied to remove speckle noises within homogeneous areas (Lee et al. 2009), resulting in smoother images with rectangular pixel shapes. Range-doppler terrain correction was employed to minimize terrain-related error using a 1-arc Shuttle Radar Topographic Mission (SRTM) Digital Elevation Model (DEM). The pixel size was resampled to 10 m to match the spatial resolution of Sentinel-2 images and subsetted to the study site.

2.2.2. Sentinel-2 optical images

Sentinel-2 images are open-access data provided by Sentinel-2A and Sentinel-2B satellite constellations. Onboard the satellites are optical Multi-Spectral Imager (MSI) instruments that record Earth's surfaces in 12 spectral bands images with spatial resolutions of 10, 20, and 60 m ranging from visible to shortwave infrared spectrum. Each satellite has a revisit capability of 10 days. The Sentinel-2 Level-2A products covering the study site were obtained from the Copernicus Open Access Hub for 2017 to 2021 based on the lowest cloud cover percentage with acquisition dates close to Sentinel-1 image acquisition for each year. The Level-2A product is geometric and atmospheric corrected products with each pixel representing surface reflectance value, hence no further preprocessing is applied (European Space Agency 2015). Only four spectral bands with native 10 m spatial resolution were used in this study, which are band Blue (B2 - 490 nm), Green (B3 - 560 nm), Red (B4 - 665 nm), and Near-Infrared (B8 - 842 nm).

2.2.3. Reference data for training

With the requirement of CNN algorithms for satellite image classification to be trained based on inputs of image subsets and their corresponding labeled polygon, this study utilized a publicly available oil palm map to be used as the training polygon in deep learning classification model development. A global 10-m smallholder and

industrial oil palm plantation map for 2019 with an overall accuracy of 96% was obtained from Descals et al. (2021). From this map, both smallholder and industrial oil palm plantation typology classes were merged into a single oil palm class thus the accuracy of the reference map was assumed to be increased. Due to the absence of other land cover information in the reference datasets, they are categorized into the same class of non-oil palm. The appearance of commonly present land covers in the study area on satellite images used in this study and how they fit the binary classification scheme are shown in Figure 2.3.

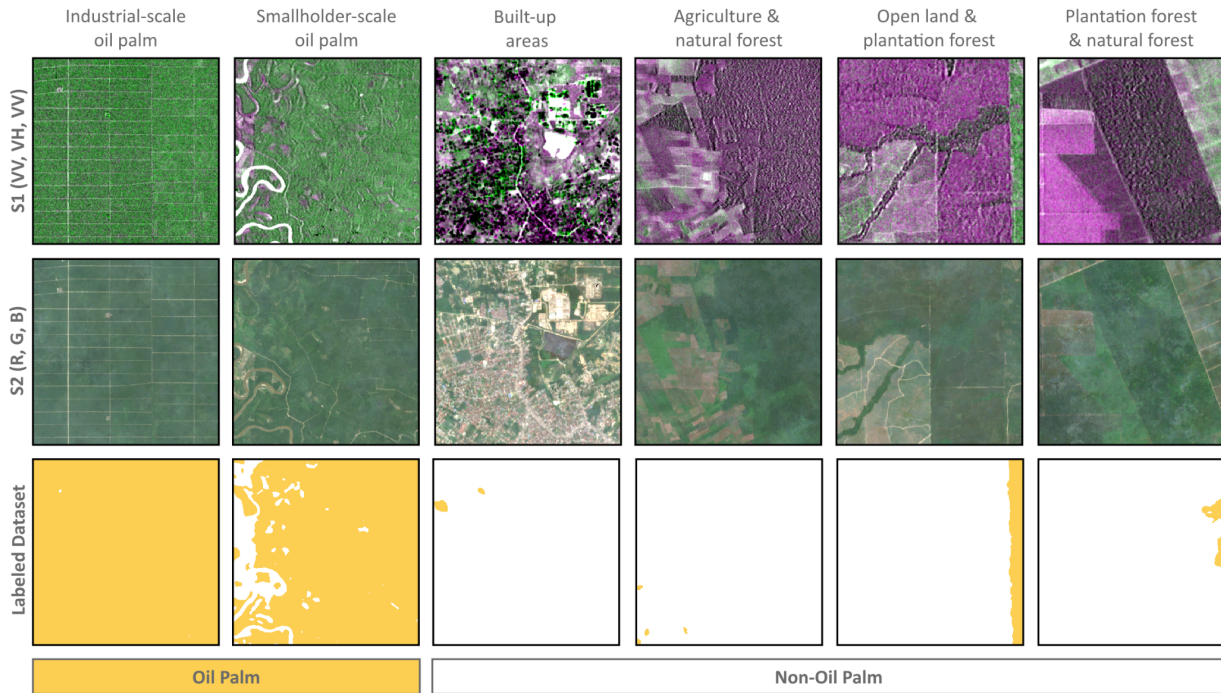


Figure 2.3. The input sample for training the classification model consisted of the labeled polygon and their corresponding satellite images showing oil palm and other dominant land covers.

2.2.4. Reference data for validation

Randomly distributed points comprised of smallholder oil palm, industrial oil palm, and non-oil palm labels were obtained from Descals et al. (2021). These points were derived from the visual interpretation of very high-resolution DigitalGlobe images (Descals et al. 2021). The two classes of oil palm typology were merged into a single oil palm class, resulting in 106 points for the oil palm class and 80 points for the non-oil palm class for assessing the accuracy of the output classification maps.

2.2.5. Ancillary data

River layers in the study area were collected from the Indonesian Ministry of Environment and Forestry. Following the Indonesian regulation, a fixed-width riparian zone layer was derived by creating a buffer within 100 m distance from the river edge. The classification for multi-temporal images to map oil palms was done within this buffer zone which is supposed to be protected areas to assess the magnitude of the violation of the law.

Additionally, Google satellite image was used to visually compare the classification outputs. This comparison was used as the means to qualitatively assess the model performance and further investigate the potential source of error beyond accuracy metrics.

2.3. Computing Infrastructure and Software

Geospatial Computing Platform is a high-performance computer facility developed and operated by the Center of Expertise in Big Geodata Science, Faculty of ITC, University of Twente. The PowerEdge R730 computing unit with 72 vCPU Intel x86-64 bit, 768 GB RAM, and NVIDIA RTX A4000 GPU was used to train CNN models and apply the model to classify the images. The CNN models were developed using Tensorflow 2.10 version and Complex-Valued Neural Network (CVNN) version 1.2.22 (Barrachina 2021).

3. METHODS

This chapter is divided into two sections, which are (3.1) Training data preparation, (3.2) Classification model development, and (3.3) Multi-year oil palm mapping on river banks. Figure 3.1 presents the overall workflow of this study.

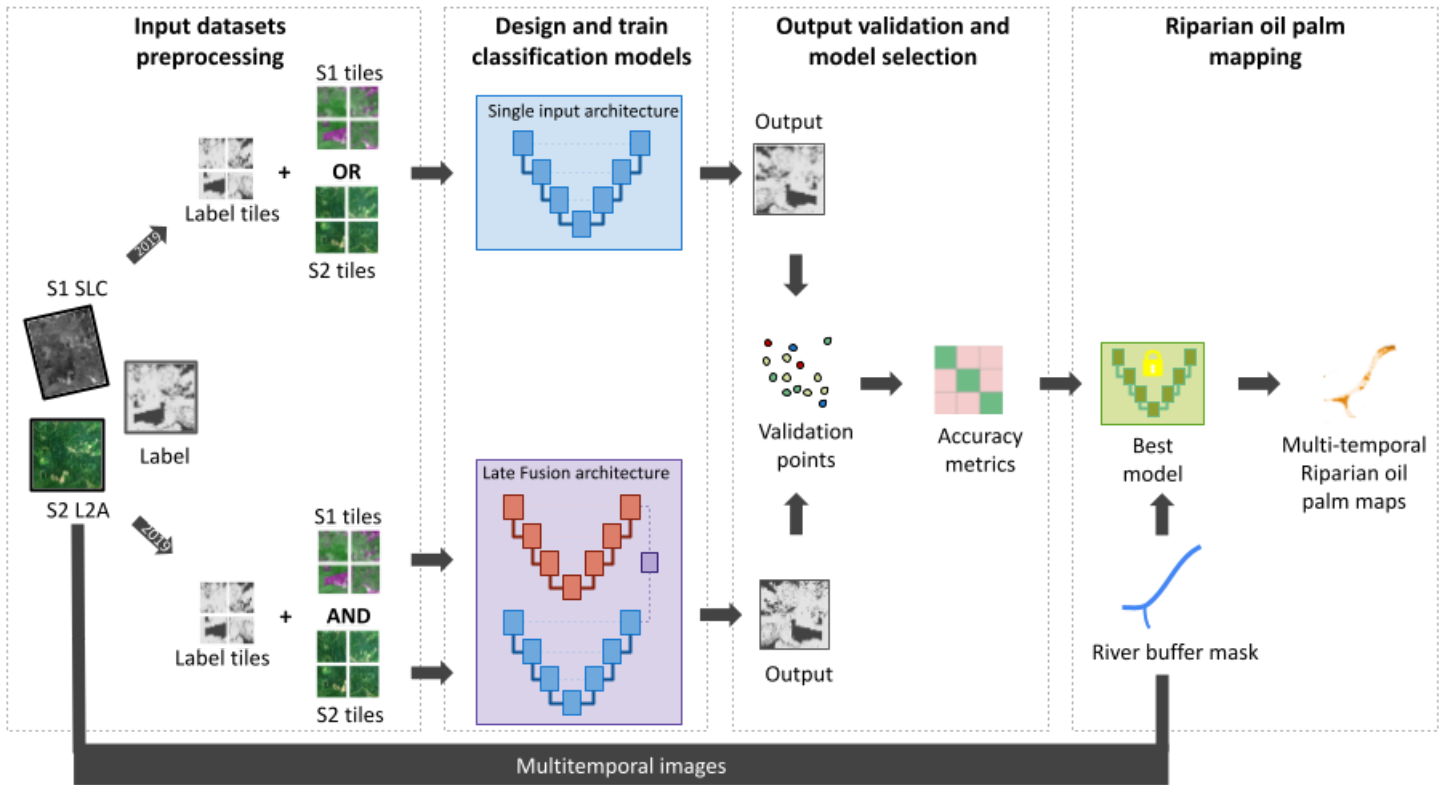


Figure 3.1. The overall workflow of the study.

3.1. Training data preparation

The preprocessed satellite images acquired in 2019 and the corresponding reference map of the same year over the study area were subsetting and divided into tiles categorized as training and evaluation datasets. This division is to ensure that the deep learning model trained on the training dataset would also perform well in classifying previously unseen data during the training from the independent evaluation dataset, by optimizing the hyperparameters, which are further detailed in subsection 3.2.5. Each tile was further cropped into smaller pairs of satellite images and reference maps, addressed as patches, with the size of 256 x 256 pixels of 10 m pixel-sized raster to accommodate memory constraints and assumed to be the optimum receptive field size for the oil palm classification task using CNN. The number of patches used for training is 1787, while the number of patches used for evaluation is 529. Figure 3.2 illustrate the division of the datasets for training the classification model.

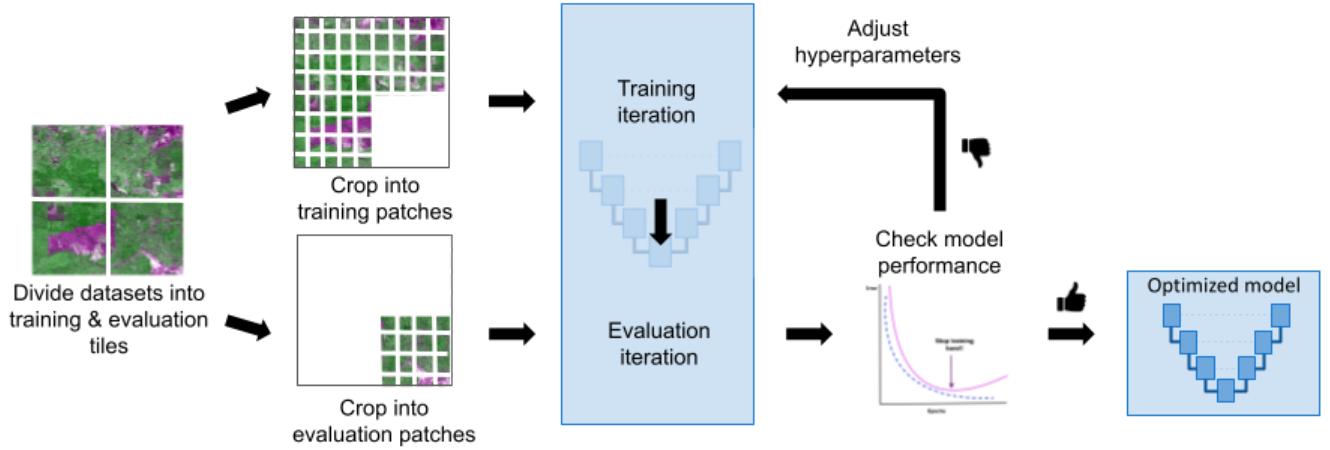


Figure 3.2. The datasets to train the model are divided into training patches ($n = 1787$) and evaluation patches ($n = 529$). The evaluation dataset was used to check the model performance on unseen data and adjust hyperparameters.

3.2. Classification model development

In this study, a deep learning-based multi-modal late fusion classification model was proposed specifically designed to handle the complex-valued polarimetric representation of Sentinel-1 SAR images and Sentinel-2 optical images. The model architecture is based on the popular UNet framework. To assess the performance of the proposed classification model, it was compared against several baseline models. The first and second baseline model is a real-valued UNet that takes input from a single modality, each with SAR or optical images. The third baseline model is a complex-valued UNet that also operates on a single modality input. Finally, a real-valued UNet model with late fusion and multi-modalities input was constructed, mimicking the structure of the proposed model. Table 3.1 provides a summary of the deep learning classification models developed in this study, along with the corresponding input images used for each model.

Table 3.1. List of deep learning classification models developed in this study

Classification Model	Input source	Representation	Data type
UNet S1	Sentinel-1 SAR	VV & VH intensity	Real
UNet S2	Sentinel-2 optical	Visible-NIR surface reflectance bands	Real
UNet Late Fusion	Sentinel-1 SAR	VV & VH intensity	Real
	Sentinel-2 optical	Visible-NIR surface reflectance bands	
Complex-valued UNet S1	Sentinel-1 SAR	Polarimetric covariance matrix	Complex
Proposed Complex-valued UNet Late Fusion	Sentinel-1 SAR	Polarimetric covariance matrix	Complex
	Sentinel-2 optical	Visible-NIR surface reflectance bands	

3.2.1. UNet

This study adopted a modified version of UNet architecture with four hidden layers (Figure 3.3). This is one hidden layer less from standard UNet architecture which was meant to accommodate memory constraints. Each

convolutional layer was followed by batch normalization and Rectified Linear Unit (ReLU) activation functions. As the network progresses towards the end, a convolutional layer with a filter size of 1 x 1 and a sigmoid activation function was applied. For this study, the UNet was trained separately using real-valued Sentinel-1 SAR images and Sentinel-2 optical images, resulting in the development of two distinct classification models.

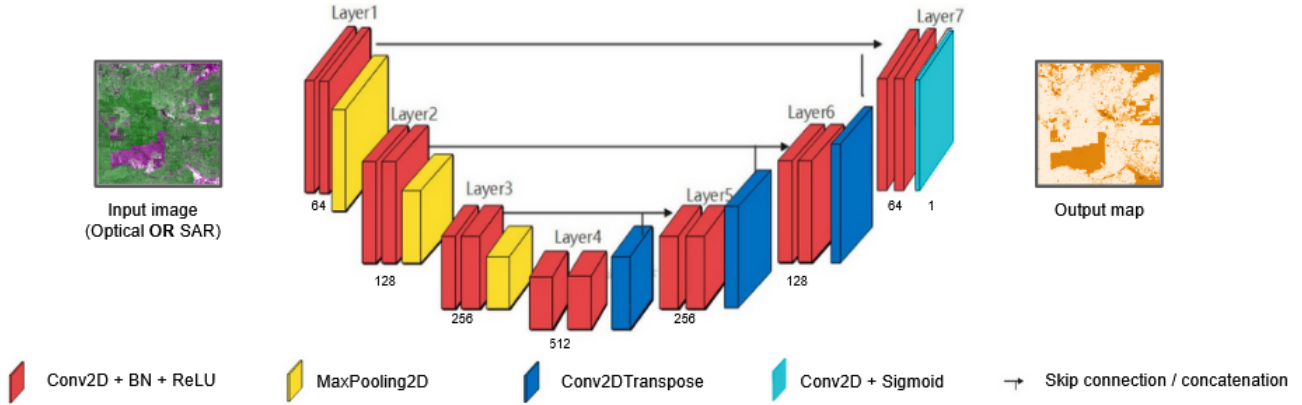


Figure 3.3. UNet architecture (Modified from Cai et al. 2022)

3.2.2. UNet with Late Fusion

UNet with Late Fusion architecture was constructed based on the work by Hafner et al. (2021). It consists of two parallel UNet networks, each tailored to process images from different modalities. Specifically, one UNet network was dedicated to optical images, while the other handles real-valued SAR images. The structure of each UNet branch follows the description provided in subsection 3.2.1.

At the end of each UNet branch, a fusion step was incorporated to combine the learned features from SAR and optical branches (Figure 3.4). The fusion was achieved through concatenation, which merges the feature maps obtained from both branches. Subsequently, three additional convolutional layers were employed, followed by a sigmoid activation function. To train this network, the Sentinel-2 optical data is utilized, along with real-valued Sentinel-1 SAR data represented by VV and VH polarization images.

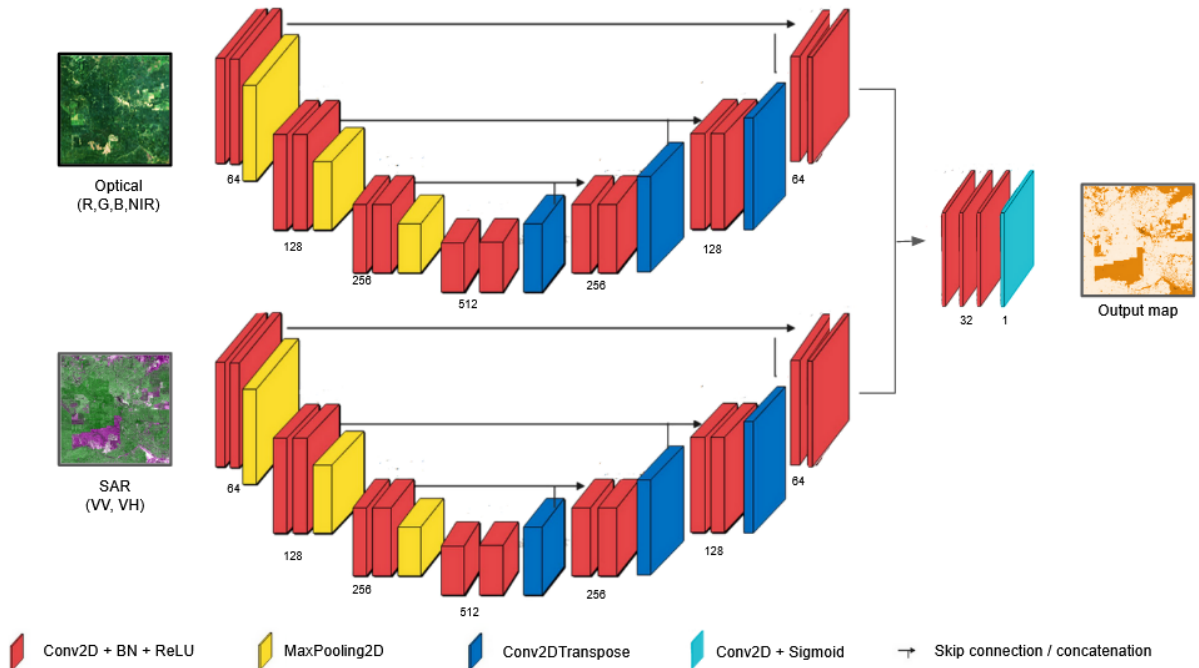


Figure 3.4. UNet with Late Fusion architecture (Modified from Cai et al. 2022)

3.2.3. Complex-valued UNet

Complex-valued UNet is a network with architecture equivalent to UNet described in subsection 3.2.1. However, it was specifically designed to handle complex-valued inputs without the need for casting values to real numbers following Barracchina et al. (2022). The main distinction lies in the replacement of regular convolutional layers with complex convolutional layers.

Complex batch normalization and complex ReLU activation functions follow each complex convolutional layer to ensure the effective handling of complex-valued features. However, the final activation function is set to return a real value to generate an output map. To train the Complex-valued UNet, a real-valued loss function is utilized, which allows the use of common optimizers during the training process (Barracchina et al. 2022a). In this study, the Complex-valued UNet was employed to train a complex-valued polarimetric covariance matrix derived from Sentinel-1 SAR images.

3.2.4. Complex-valued UNet with Late Fusion

Complex-valued UNet with Late Fusion is a network with architecture equivalent to UNet with Late Fusion described in subsection 3.2.2. The incorporation of two parallel branches is dedicated to processing input from a specific modality. One branch processes the complex-valued SAR images, while the other branch handles the optical images cast as complex-valued with an imaginary part of zero. These branches follow the structure of the Complex-valued UNet described in subsection 3.2.3.

At the end of each branch, the learned features from SAR and optical branches are fused using a concatenation operation. Following the fusion step, three additional convolutional layers were applied to further refine the combined features. Finally, a sigmoid activation function is used to generate an output map, representing the classification results based on the fused features.

3.2.5. Hyperparameters

The learning process of deep learning classification models is influenced by hyperparameters, which are parameters responsible for regulating the behavior of a training algorithm. Determining the optimal values for these hyperparameters is crucial to ensure the development of high-performing models with good generalization abilities for a specific task (Prince 2023). The model with optimal hyperparameters, referred to as the optimized model, can be indicated by low loss function value and high accuracy scores, both during training and evaluation using unseen datasets which are deemed to be favorable results. Such criteria were achieved for all models by using the following hyperparameters:

- **Number of epochs (50)**, depicts the amount of time the entire training dataset is passed to the network
- **Batch size (10)**, represents the number of samples passed to the network in an iteration
- **Learning rate (1e-5)**, which is the rate of the network to update its parameters towards optimum weights
- **Optimizer (Adam)**, a function that adapts the learning rate and weights to reduce loss and improve accuracy
- **Early stopping (30 epochs)**, a safeguard to avoid overfitting by stopping the training and keeping the best model after the loss metric over the evaluation dataset does not decrease in several iterations
- **Loss function (Binary Cross Entropy)**, measures the goodness of the algorithm in classifying features into target class

3.2.6. Model validation

Each trained deep learning model was used to classify images from the year 2019. The output maps from each model were compared against 186 validation points where confusion matrices were created and accuracy metrics were calculated. In a binary classification scheme used in this study, True Positive (TP) refers to the amount of correctly classified pixels of the main target class, which is oil palm. On the other hand, True Negative (TN) refers to the number of non-oil palm pixels which are correctly classified. False Positive (FP) represents the number of non-oil palm pixels that are misclassified as oil palm, while False Negative (FN) represents the amount of oil palm pixels that are misclassified as non-oil palm. The following metrics were further calculated for accuracy assessment (Knudby 2021):

- Producer's Accuracy, also known as Recall, refers to the probability of a class on the validation dataset is correctly predicted in the classification output. Recall is obtained by dividing the number of correctly classified pixels in a certain class (true positive) by the total number of pixels on the validation dataset belonging to that class:

$$Recall = \frac{n \text{ correctly classified pixel of a class}}{n \text{ validation sample of a class}} \quad (3.1)$$

- User's Accuracy, also known as Precision, refers to the probability of a predicted class being literally that class on the validation dataset. Precision is obtained by dividing the number of correctly classified pixels in a certain class by the total number of pixels classified in the same class:

$$Precision = \frac{n \text{ correctly classified pixel of a class}}{n \text{ pixel classified as that class}} \quad (3.2)$$

- F1-score, which is a harmonic mean of Precision and Recall and can be calculated by the following equation for each class:

$$F1 \text{ score} = 2 \times \frac{(Precision \times Recall)}{(Precision + Recall)} \quad (3.4)$$

F1-score metric addresses the first research question and was used as the deciding factor for selecting the most accurate model to be applied to the multi-temporal image classification of oil palm in the study area for the year 2017 to 2021.

3.3. Multi-year mapping of oil palm on river banks

After evaluating the accuracy metrics, the best-performing model was selected for classifying images captured in 2017, 2018, 2019, 2020, and 2021, resulting in the creation of annual oil palm maps covering a five-year period. Prior to classification, the images were cropped to a fixed-width area within river banks, determined by applying a 100 m buffer from each river edge using river layers. Since validation points were only available for 2019 from Descals et al. (2021), direct validation of the maps generated for other years was not possible. However, a qualitative assessment was conducted by visually examining the distribution and occurrence of oil palm along rivers throughout the years. To address the second research question, the extent of multi-temporal oil palm presence along river banks was summarized and presented in both a map and a bar chart for better visual interpretation.

4. RESULTS

This chapter is divided into two sections. Section 4.1. describes the results of the deep learning classification model outputs' accuracy assessment for oil palm mapping. Section 4.2. explains the distribution and areas of oil palm plantations on riparian zones over a five-year period produced by applying the best classification model to multi-temporal images.

4.1. Deep learning classification model outputs

Table 4.1 shows the results of the accuracy assessment from each classification model output. It can be seen that the classification model trained using Sentinel-2 optical images resulted in the lowest number of correctly classified pixels for oil palm (TP) and non-oil palm classes (TN). Consequently, it also provides classification output with the highest misclassification rate. On the other hand, the classification models trained by involving Sentinel-1 SAR image representation outperform the model trained only with optical images and consistently delivered higher correctly classified pixels for both oil palm and non-oil palm classes with more than a half reduction of the misclassification rate.

Table 4.1. Accuracy metrics for each classification output. CV-UNet S1 yields the highest accuracy while UNet S2 yields the least accuracy.

Classification	TP	TN	FP	FN	Precision	Recall	F1-score
UNet S1	100	78	6	2	0.943	0.980	0.962
UNet S2	93	66	13	14	0.877	0.869	0.873
UNet Late Fusion	100	79	6	1	0.943	0.990	0.966
CV-UNet S1	103	77	3	3	0.972	0.972	0.972
CV-UNet Late Fusion	102	78	4	2	0.962	0.981	0.971

TP: Correctly classified oil palm (True Positive)

FP: Non-oil palm classified as oil palm (False Positive)

TN: Correctly classified non-oil palm (True Negative)

FN: Oil palm classified as non-oil palm (False Negative)

Utilization of complex-valued neural networks to process complex-valued images slightly improves the rate of correctly classified pixels compared to their equivalent real-valued neural network model. This was achieved by a reduction in misclassification from the non-oil palm class to the oil palm class, represented by the higher Precision values from complex-valued models compared to their real-valued counterparts. However, the rate of misclassification from the oil palm class to the non-oil palm class seemed to be slightly higher in the complex-valued models, as suggested by their lower Recall values compared to their real-valued equivalence.

The highest F1-score was obtained from CV-UNet trained with the complex-valued representation of Sentinel-1 SAR images with an F1-score of 0.972. This model is considered the best model because it is able to classify many palm pixels correctly and has a relatively lower and balanced misclassification rate for false positive and false negative cases compared to other models. For that reason, this model was chosen to classify multi-temporal images of complex-valued Sentinel-1 SAR images to map oil palm plantations along rivers.

4.2. Oil palm plantations on the riparian zone

Using the assumption that riparian zones are defined as the river bank area of both sides of the rivers within 100 m distance, the estimated total area of riparian zones in the study area sums up to 28,420 hectares. Figure 4.3

shows the portions of riparian zones occupied by oil palm plantations. It can be clearly seen that there is an increasing trend of oil palm plantation occurrence in the riparian zones throughout the study period.

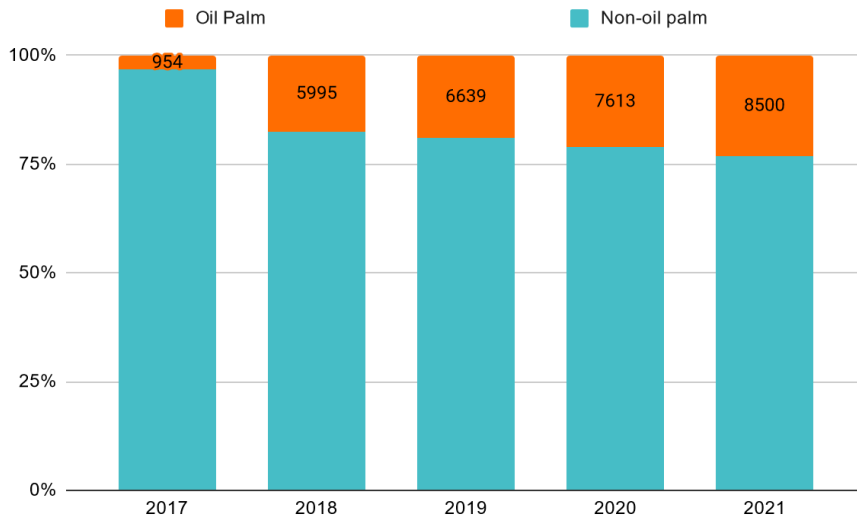


Figure 4.3. The increasing oil palm plantation occupancy area on riparian zones from 2017 to 2021. The presented oil palm plantation areas are in hectares units.

At the start of the study period, oil palm plantations covered roughly 954 hectares, accounting for approximately 3% of the riparian zone area. There was a significant change in oil palm plantations area from 2017 to 2018, with the area increasing almost sevenfold to 5,995 hectares. Following this surge, the area continued increasing steadily with an average of nearly 4%. This has led to a cumulative oil palm plantation occupancy of 8,500 hectares by 2021, which accounted for 29% of the riparian zone areas.

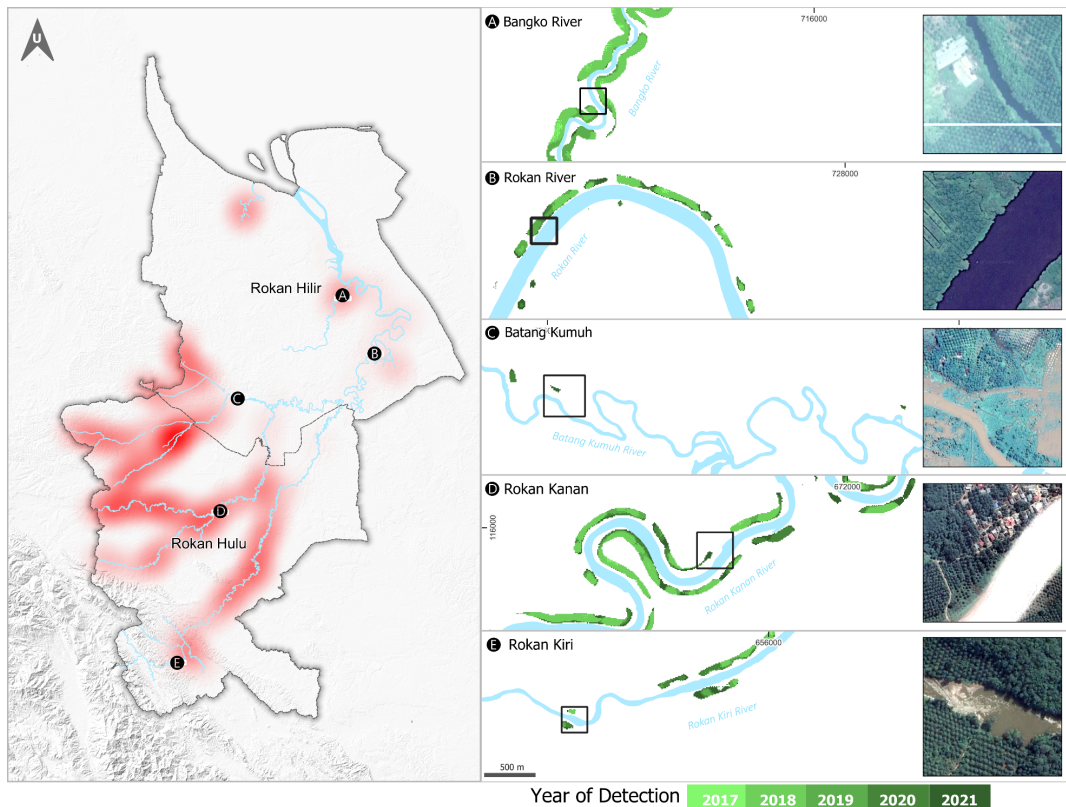


Figure 4.4. Heatmap of oil palm plantations located on river banks (left) and sample locations of detected oil palm plantations from five main rivers in the study area complimented with Google satellite image view (right).

Figure 4.4 depicts the distribution of oil palm plantations within the riparian zone of the study area. From the heatmap, it can be seen that the majority of the oil palm planted along rivers is located in Rokan Hulu Regency. This region is passed by three major rivers, which are Rokan Kiri, Rokan Kanan, and Batang Kumuh Rivers. The upstream part of the Rokan Kiri River, located in the southernmost part of the study area, is characterized by mountainous terrain, which accounts for the absence of oil palms in that particular area. However, oil palm plantations can be found immediately after the change in elevation (Figure 4.4.E).

While the upstream region of the study area exhibits a dense oil palm plantation occupancy within the riparian zones, there is a noticeable decrease in plantation coverage towards the middle region of the study area. This border region between Rokan Hulu Regency and Rokan Hilir Regency is the confluence location of major rivers. This condition has made this area prone to flooding, as Figure 4.4.C illustrates the absence of oil palm plantations in what appears to be floodplain areas.

The distribution of oil palm plantations within the riparian zone appears to be well-captured by the classification model as depicted in Figure 4.4. However, there are some cases where certain oil palm plantations are omitted from the classification. Such omission error mainly occurs on open-canopy oil palm plantations. Figure 4.5 shows such a problem when the classification map from the year 2021 was overlaid with the high-resolution Google satellite image.

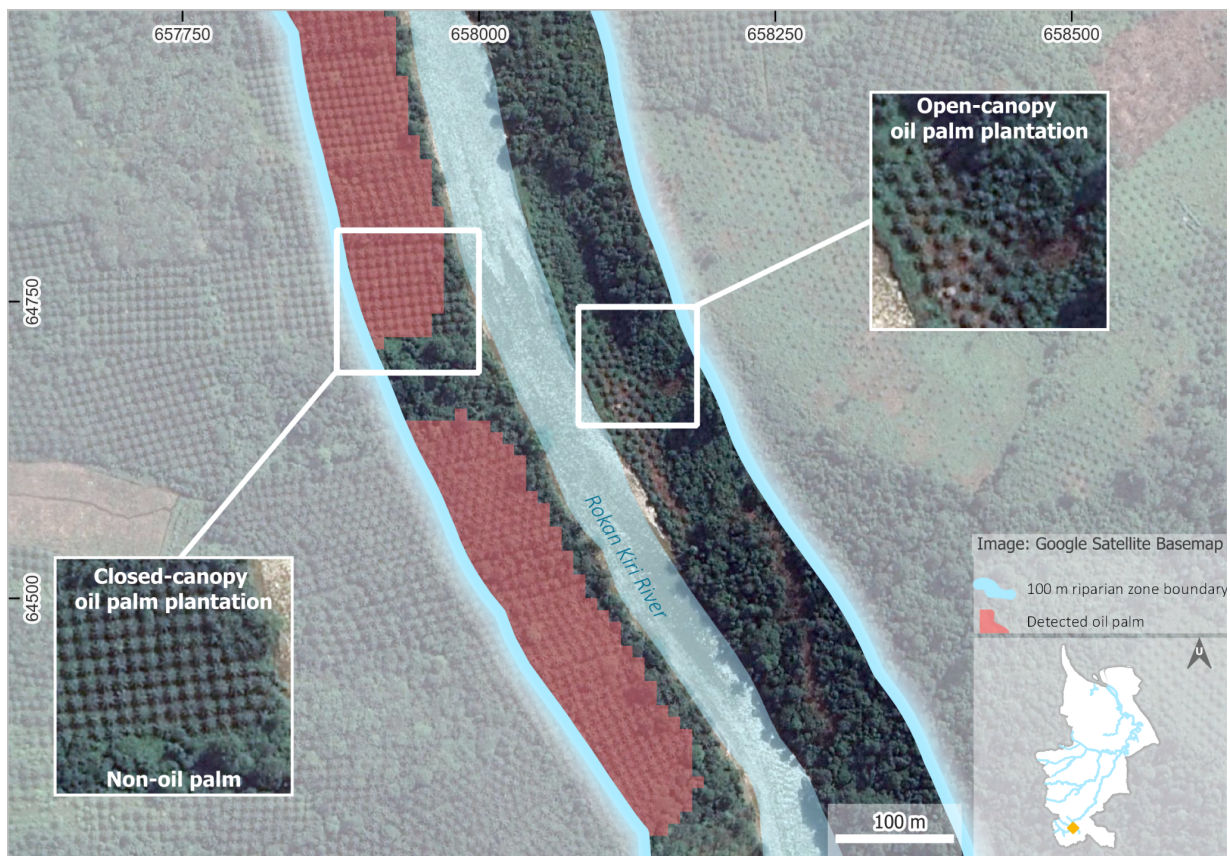


Figure 4.5. Detected oil palm in 2021 within the riparian zone. The classification model omitted open-canopy oil palm plantations which typically are young and immature plantations.

5. DISCUSSION

In this study, a neural network classification model that enables the fusion of complex-valued SAR images and optical images was proposed for oil palm mapping. Although the F1-score obtained from the proposed model was higher in comparison with other tested real-valued methods (i.e. UNet S1, UNet S2, or UNet Late Fusion), it was slightly lower than the CV-UNet trained only with complex-valued Sentinel-1 SAR images. The difference in F1-score between each classification model trained with SAR images, either real-valued or complex-valued, was less than 1%. This finding confirms the result from several studies (Barrachina et al. 2022a, 2022b; Mulissa et al. 2019) which found only a small increase in land cover mapping accuracy when complex-valued architecture and complex-valued SAR representation were used in comparison to their real-valued equivalent neural network and inputs. However, it should be noted that Sentinel-1 SAR images used in this study have only two polarizations which hinder the data to be transformed into more polarimetric representations that might be more beneficial in differentiating scatterers and more suitable for complex-valued neural networks as compared to other SAR datasets with quad polarizations (Barrachina et al. 2022b). Such datasets are not always available i.e. not distributed as open data or not covering major regions of the earth's surface.

The time required to train a complex-valued neural network classification model was approximately five times longer than its real-valued equivalent model. This factor already outweighs the little accuracy improvement benefit a complex-valued neural network could offer in the oil palm classification task. Previous studies have only experimented with complex-valued neural network architectures for the benchmark regions where quad polarization SAR datasets are available (Mulissa et al. 2019, Barrachina et al. 2022a, 2022b). This suggests that a complex-valued neural network is not practical to be applied in scale. Conversely, preprocessed Sentinel-1 SAR images are available on popular geospatial cloud computing platforms which simplify the processing pipeline while working with UNet to achieve similar accuracy offered by complex-valued network counterparts.

The UNet classification model trained with Sentinel-2 optical images yielded the lowest accuracy as compared to other models trained with Sentinel-1 SAR images. The four 10 m spectral bands in the visible and near-infrared spectrum used in the classification might not be sufficient in differentiating spectral properties from different tree covers. Tree covers such as oil palm can be difficult to differentiate from plantation forests for wood fibers and rubbers which are commonly present in the study area (Sarzynski et al. 2020). Involving spectral bands beyond the near-infrared region might add the capability to distinguish these objects but with the trade-off of reduction of spatial resolution to 20 m (Nomura et al. 2019, Descals et al. 2023). On the other hand, Sentinel-1 SAR images alone were able to distinguish oil palm plantations from non-oil palm as suggested by the accuracy assessment results from classification models trained with Sentinel-1 SAR images involvement.

As there was only a small increase in accuracy obtained when both optical and SAR images were used in the UNet Late Fusion model, it suggests that most of the benefits in the oil palm classification were gained from the SAR data. Previous studies found that using SAR images alone contributed to the highest accuracy of the oil palm class as compared to other classification inputs including optical and SAR image fusions (Cheng et al. 2016, Monzalve-Tellez 2022). Descals et al. (2021) only used a red band from Sentinel-2 optical images in addition to VV and VH polarization images from Sentinel-1. The red band shows the harvest road pattern in industrial oil palm plantations well and was essential in differentiating and mapping industrial and smallholder oil palm plantations automatically using CNN (Descals et al. 2021). This could mean that a certain optical image band might only be necessary when such a highly specific task to perform oil palm classification to typology level is the objective. In the region where oil palms are grown and cloud cover are massive, using Sentinel-1 alone might be sufficient to map oil palm with a simple classification scheme as presented in this study.

While closed-canopy oil palm can be effectively detected from SAR images due to the distinct backscattered signal as compared to other tropical plantations (Miettinen & Liew 2011), it might be difficult to map open-canopy oil palm plantations which typically are young plantations under three years. Such a problem was also found in this study upon comparing the oil palm map produced from this study to a high-resolution Google satellite image. With this limitation, the area of oil palm plantations within the riparian zones should be carefully interpreted as solely productive oil palm plantations indicated by their closed-canopy characteristic. The previously reported rapid change of oil palm plantations within the riparian zones from 2017 to 2018 in Section 4.2 might not represent the new plantation establishment. Rather, it could be interpreted as the plantations that were already there but were just detected in 2018 as the plantations matured and formed closed-canopy.

Due to the limitation of detecting open-canopy oil palm plantations, previous studies have only included closed-canopy oil palm plantations in their classification scheme (Koh et al. 2011, Descals et al. 2021). Combining closed-canopy oil palm plantations and open-canopy oil palm plantations into a single class might cause misclassification problems, which could be mitigated by separating these plantation types into separate classes in the classification (Descals et al. 2019). Post-classification correction using visual interpretation to manually digitize open-canopy oil palm plantations was also demonstrated when high-resolution optical images are available (Miettinen et al. 2018, Gaveau et al. 2022).

This study used deep learning classification models to map oil palm which requires a large number of samples to be trained with. Therefore, the availability of an oil palm map with high accuracy from Descals et al. (2021) was essential and reduced the necessity for manually digitizing polygons to train the deep learning model. As the reference map used for training classification models in this study was limited to closed-canopy oil palm plantations, the problem with the omission of open-canopy plantations was expected. Such a problem could have been avoided with additional training polygons that cover open-canopy plantations. However, manual digitization to create open-canopy oil palm plantation training polygons was not implemented due to the unavailability of high-resolution optical images with clear acquisition data to aid the visual interpretation and match the image acquisition date to be classified. Additionally, a large number of samples to include open-canopy oil palm class into the classification scheme used by the deep learning model may be required which could have been a tremendous task to perform with manual digitization. A previous similar study (Muzakki 2021) suffered from low mapping accuracy due to the low number of samples despite data augmentation being employed, but this could also be due to poor sample quality with training data labeling only aided with medium resolution images.

The classification model developed in this study is applicable to the dataset beyond which it was trained, which are multi-temporal SAR images acquired in years other than 2019. The quantitative accuracy assessment, however, could only be done to the map for the year 2019 due to the availability of the validation points. Despite so, from a visual assessment of each year's classification map, it was found that the area detected as oil palm in the previous years was also detected as oil palm in the later years. The increasing trend found in this study is consistent with several publications (Numata et al. 2022, BPS-Statistics Indonesia 2019) stating the increase of oil palm areas in Riau, despite not specifically in riparian zones.

Reflecting on the examples above, it can be said that UNet classification model trained with SAR images is promising to map oil palms in riparian areas using open data and platforms. Currently, the Indonesian government still relies on the manual digitization of commercial high-spatial resolution optical images to map oil palm plantation distribution (AURIGA 2019). Such a method could be time-consuming and would only provide non-actual information as the land cover might have already changed by the time a cloud-free image mosaic was obtained. While the adoption of advanced remote sensing methods in the public sector might take a long time to come, the information on the distribution of oil palm on the river banks resulting from this study can be used to aid law enforcement as well as considerations for taking preventive steps so that violations do not spread to other borders that have not yet been planted with oil palm. One of the preventive measures is to define the protected

areas into spatially explicit zoning regulation in spatial planning as the safeguard for permits for proposed land use activities (Budiman et al. 2020). Despite being mandated by Indonesian Spatial Planning Law since 2007 to establish the regional spatial plan, several Regency in Riau Province has yet to finalize their spatial plan (Media Center Riau 2023). The absence of these legal instruments, together with the lack of monitoring in the field, might be the reason why violations of planting oil palm on the river banks continue to occur.

In the private sector where advanced technology adoption is more likely to occur, sustainable certification bodies can utilize the demonstrated methods as well as the information regarding the distribution of oil palm produced in this study. Information on oil palm plantations in the riparian area can help determine which plantations meet the requirements to receive sustainable certification. Large oil palm companies that incidentally also have palm oil processing factories can also apply the approach demonstrated in this study to ensure that the palm they supply comes from sustainable plantings and does not violate the law.

Apart from enforcing the law for violation and prevention of oil palm occupation in the riparian area, information about the distribution of palm oil can also be used to determine areas for restoring riparian areas that are already planted with oil palms. The restoration can be prioritized to the area that is most suitable and beneficial in a way it can store more carbon, prevent excessive sedimentation, and brings back biodiversity that was once lost due to the presence of oil palm plantations. However, such a task of prioritization can be challenging due to the many geospatial layers required. The restoration of riparian buffers can be an opportunity for a plantation to be eligible for sustainability certification such as Roundtable Sustainable Palm Oil (RSPO) (Lucey et al. 2018).

Restoration of riparian buffers can be passively done by letting the natural regrowth of vegetation in the river banks (Lucey et al. 2018). The already planted oil palms on the riparian zone can be retained but would not be managed for productive purposes. Such treatment is to ensure the existing oil palm in the riparian area facilitates natural regrowth by providing shading (Woodham et al. 2019). In the active approach, enrichment planting can be done with tree species between oil palms in the riparian zone. Such an approach can be eligible for revenue options from green financing which might shift the dependency of smallholder farmers from unsustainable palm oil production to an agroforestry system where protection of riparian buffers is implemented (Abram et al. 2016, Budidadi et al. 2019). With the vast amount of riparian zone can potentially be restored, the location of oil palm plantations can be shift elsewhere such as in the marginal and abandoned land (Koh & Ghazoul 2010) where biodiversity is low and the introduction of plantations would not disturb the ecosystem.

6. CONCLUSION AND RECOMMENDATION

6.1. Conclusion

This study proposed a neural network model that combines complex-valued SAR and optical images. By considering the processing time and insignificant improvement of accuracy offer by complex-valued SAR or fusion with optical images, this study suggests that using UNet trained with real-valued Sentinel-1 SAR alone could provide good accuracy in oil palm mapping. The classification model developed in this study was useful in mapping oil palm distribution on the riparian zone multi-temporally, which area has increased during the period of the study from 2017 to 2021. The classification model was unable to detect open-canopy oil palm plantations.

6.2. Recommendation

Further study could focus on the development of a method to detect open-canopy oil palms from remote sensing data while maintaining high accuracy mapping for closed-canopy oil palm plantations. Beyond information extraction from satellite images, the existing oil palm distribution map can be combined with other geospatial layers to determine the suitable location for restoration in the riparian zone as well as the location where oil palm can potentially be grown sustainably.

LIST OF REFERENCES

- Abood, S. A., Lee, J. S. H., Burivalova, Z., Garcia-Ulloa, J., & Koh, L. P. (2015). Relative contributions of the logging, fiber, oil palm, and mining industries to forest loss in Indonesia. *Conservation Letters*, 8(1), 58-67.
- Abram, N. K., MacMillan, D. C., Xofis, P., Ancrenaz, M., Tzanopoulos, J., Ong, R., Goosens, B., Koh, L., P., Del Valle, C., Peter, L., Morel, A., C., Lackman, I., Chung, R., Kler, H., Ambu, L., Baya, W., & Knight, A. T. (2016). Identifying where REDD+ financially out-competes oil palm in floodplain landscapes using a fine-scale approach. *PLoS One*, 11(6), e0156481.
- AURIGA (2019). Oil palm cover in Indonesia: An analysis of satellite imagery from 2014-2016. Jakarta: Indonesia's Ministry of Agriculture, Corruption Eradication Commission (KPK), Space and Aeronautics Agency (LAPAN).
- Bakhtary, H., Haupt, F., Luttrell, C., Landholm, D., & Jelsma, I. (2021). *Promoting sustainable oil palm production by independent smallholders in Indonesia*.
- Barrachina, J. A. (2021). NEGU93/cvnn. Zenodo. <https://doi.org/10.5281/zenodo.4452131>.
- Barrachina, J. A., Ren, C., Morisseau, C., Vieillard, G., Ovarlez, J. (2022a). Comparison between equivalent architectures of complex-valued and real-valued neural networks - Application on Polarimetric SAR image segmentation. *Journal of Signal Processing Systems*.
- Barrachina, J. A., Ren, C., Vieillard, G., Morisseau, C., & Ovarlez, J. P. (2022b). Real-and Complex-Valued Neural Networks for SAR image segmentation through different polarimetric representations. In *2022 IEEE International Conference on Image Processing (ICIP)* (pp. 1456-1460). IEEE.
- Budidarsono, S., Susanti, A., & Zoomers, A. (2013). Oil palm plantations in Indonesia: The implications for migration, settlement/resettlement and local economic development. *Biofuels-economy, environment and sustainability*, 1, 173-193.
- Braun, A., & Offermann, E. (2022). Polarimetric information content of Sentinel-1 for land cover mapping: An experimental case study using quad-pol data synthesized from complementary repeat-pass acquisitions. *Frontiers in Remote Sensing*, 3, 905713.
- Budiman, H., Dialog, B. L., & Anugrah, D. (2020, December). Spatial Planning Policy in the Region: Problems and Solutions. In *The 2nd International Conference of Law, Government and Social Justice (ICOLGAS 2020)* (pp. 434-439). Atlantis Press.
- Budiadi, Susanti, A., Marhaento, H., Ali Imron, M., Permadi, D. B., & Hermudananto. (2019, October). Oil palm agroforestry: an alternative to enhance farmers' livelihood resilience. In *IOP Conference Series: Earth and Environmental Science* (Vol. 336, No. 1, p. 012001). IOP Publishing.
- BPS-Statistics Indonesia (2019). *Statistik Kelapa Sawit Indonesia 2019* [Indonesian Oil Palm Statistics 2019].
- Cai, Y., & Wang, Y. (2022, March). Ma-unet: An improved version of unet based on multi-scale and attention mechanism for medical image segmentation. In *Third International Conference on Electronics and Communication; Network and Computer Technology (ECNCT 2021)* (Vol. 12167, pp. 205-211). SPIE.
- Campbell, J. B., & Wynne, R. H. (2011). *Introduction to Remote Sensing* (5th ed.). New York: The Guilford Press.
- Carolita, I., Darmawan, S., Permana, R., Dirgahayu, D., Wiratmoko, D., Kartika, T., & Arifin, S. (2019, June). Comparison of optic Landsat-8 and SAR Sentinel-1 in oil palm monitoring, case study: Asahan, North Sumatera, Indonesia. In *IOP Conference Series: Earth and Environmental Science* (Vol. 280, No. 1, p. 012015). IOP Publishing.
- Carlson, K.M., Curran, L.M., Ponette-González, A.G., Ratnasari, D., Lisnawati, N., Purwanto, Y., Brauman, K.A. & Raymond, P.A. (2014). Influence of watershed-climate interactions on stream temperature, sediment yield, and metabolism along a land use intensity gradient in Indonesian Borneo. *Journal of Geophysical Research: Biogeosciences*, 119(6), 1110-1128.
- Chemura, A., van Duren, I., & van Leeuwen, L. M. (2015). Determination of the age of oil palm from crown projection area detected from WorldView-2 multispectral remote sensing data: The case of Ejisu-Juaben district, Ghana. *ISPRS journal of photogrammetry and remote sensing*, 100, 118-127.
- Cheng, Y., Yu, L., Cracknell, A. P., & Gong, P. (2016). Oil palm mapping using Landsat and PALSAR: A case study in Malaysia. *International journal of remote sensing*, 37(22), 5431-5442.
- Cheng, Y., Yu, L., Xu, Y., Lu, H., Cracknell, A. P., Kanniah, K., & Gong, P. (2018). Mapping oil palm extent in Malaysia using ALOS-2 PALSAR-2 data. *International Journal of Remote Sensing*, 39(2), 432-452.
- Choong, K. L., Kanniah, K. D., Pohl, C., & Tan, K. P. (2017). A review of remote sensing applications for oil palm studies. *Geo-spatial Information Science*, 20(2), 184-200.
- Corley, R. H. V. (2009). How much palm oil do we need?. *Environmental Science & Policy*, 12(2), 134-139.

- Danylo, O., Pirker, J., Lemoine, G., Ceccherini, G., See, L., McCallum, I., Kraxner, F., Achard, F. & Fritz, S. (2021). A map of the extent and year of detection of oil palm plantations in Indonesia, Malaysia and Thailand. *Scientific data*, 8(1), 1-8.
- Darmawan, S., Carolita, I., & Ananta, E. (2020, June). Identification of oil palm plantation on multiscatter and resolution of SAR data using variety of classifications algorithm (case study: Asahan District, North Sumatera Province). In *IOP Conference Series: Earth and Environmental Science* (Vol. 500, No. 1, p. 012075). IOP Publishing.
- Darto, M [@dartowojtyla]. (2023, June 23). *Expansion of oil palm, its claim for the welfare of rural communities. The proof: Only 21.22% of oil palm companies build plasma as regulated by the Government or only around 580 comply with plasma construction from around 2,864 plantation companies* [Tweet]. Twitter. <https://twitter.com/dartowojtyla/status/1672258478336012288>
- Decamps, H., Naiman, R.J., McClain, M.E. (2009). Riparian Zones. In Likens, G. E. (Ed.). *Encyclopedia of inland waters* (pp. 396-403). Elsevier.
- Descals, A., Szantoi, Z., Meijaard, E., Sutikno, H., Rindanata, G., & Wich, S. (2019). Oil palm (*Elaeis guineensis*) mapping with details: smallholder versus industrial plantations and their extent in Riau, Sumatra. *Remote Sensing*, 11(21), 2590.
- Descals, A., Wich, S., Meijaard, E., Gaveau, D. L., Peedell, S., & Szantoi, Z. (2021). High-resolution global map of smallholder and industrial closed-canopy oil palm plantations. *Earth System Science Data*, 13(3), 1211-1231.
- Descals, A., Wich, S., Szantoi, Z., Struebig, M. J., Dennis, R., Hatton, Z., Ariffin, T., Unus, N., Gaveau, D. L. A., & Meijaard, E.: High-resolution global map of closed-canopy coconut, *Earth Syst. Sci. Data Discuss.* [preprint], <https://doi.org/10.5194/essd-2022-463>, in review, 2023.
- Dong, R., Li, W., Fu, H., Gan, L., Yu, L., Zheng, J., & Xia, M. (2019). Oil palm plantation mapping from high-resolution remote sensing images using deep learning. *International Journal of Remote Sensing*, 41(5), 2022-2046.
- European Space Agency (2015). *Sentinel-2 User Handbook*.
- European Space Agency (2022, October 11). *Sentinel-1 SAR User Guide*. <https://sentinel.esa.int/web/sentinel/user-guides/sentinel-1-sar>
- Gao, F., Huang, T., Wang, J., Sun, J., Hussain, A., & Yang, E. (2017). Dual-branch deep convolution neural network for polarimetric SAR image classification. *Applied Sciences*, 7(5), 447.
- Gaveau, D. L., Sheil, D., Husnayaen, Salim, M. A., Arjasakusuma, S., Ancrenaz, M., Pacheco, P., & Meijaard, E. (2016). Rapid conversions and avoided deforestation: examining four decades of industrial plantation expansion in Borneo. *Scientific reports*, 6(1), 32017.
- Gaveau, D.L., Locatelli, B., Salim, M.A., Manurung, T., Descals, A., Angelsen, A., Meijaard, E. and Sheil, D. (2022). Slowing deforestation in Indonesia follows declining oil palm expansion and lower oil prices. *PLoS one*, 17(3), e0266178.
- Giam, X., Hadiaty, R.K., Tan, H.H., Parenti, L.R., Wowor, D., Sauri, S., Chong, K.Y., Yeo, D.C. & Wilcove, D.S. (2015). Mitigating the impact of oil-palm monoculture on freshwater fishes in Southeast Asia. *Conservation Biology*, 29(5), 1357-1367.
- Government Regulation No. 35 (1991). *Rivers*. Indonesian government. Accessible from: <https://peraturan.bpk.go.id/Home/Details/58175>
- Gray, R. E., Slade, E. M., Chung, A. Y., & Lewis, O. T. (2019). Movement of moths through riparian reserves within oil palm plantations. *Frontiers in Forests and Global Change*, 2, 68.
- Hajnsek, I., & Desnos, Y. L. (Eds.). (2021). *Polarimetric synthetic aperture radar: principles and application* (Vol. 25). Springer Nature.
- Hansen, J. N., Mitchard, E. T., & King, S. (2020). Assessing forest/non-forest separability using Sentinel-1 C-band synthetic aperture radar. *Remote Sensing*, 12(11), 1899.
- Hidayat, K. N., Glasbergen, P., & Offermans, A. (2015). Sustainability certification and palm oil smallholders' livelihood: A comparison between scheme smallholders and independent smallholders in Indonesia. *International Food and Agribusiness Management Review*, 18(1030-2016-83041), 25-48.
- Horton, A. J., Lazarus, E. D., Hales, T. C., Constantine, J. A., Bruford, M. W., & Goossens, B. (2018). Can riparian forest buffers increase yields from oil palm plantations? *Earth's Future*, 6(8), 1082-1096.
- Ivancic, H., & Koh, L. P. (2016). Evolution of sustainable palm oil policy in Southeast Asia. *Cogent Environmental Science*, 2(1), 1195032.
- Jelsma, I., Schoneveld, G. C., Zoomers, A., & van Westen, A. C. (2017). Unpacking Indonesia's independent oil palm smallholders: an actor-disaggregated approach to identifying environmental and social performance challenges. *Land use policy*, 69, 281-297.
- Kemker, R., Salvaggio, C., & Kanan, C. (2018). Algorithms for semantic segmentation of multispectral remote sensing imagery using deep learning. *ISPRS journal of photogrammetry and remote sensing*, 145, 60-77.

- Khasanah, N. M., van Noordwijk, M., & Ningsih, H. (2015). Aboveground carbon stocks in oil palm plantations and the threshold for carbon-neutral vegetation conversion on mineral soils. *Cogent Environmental Science*, 1(1), 1119964.
- Koh, L. P. (2008). Can oil palm plantations be made more hospitable for forest butterflies and birds?. *Journal of Applied Ecology*, 45(4), 1002-1009.
- Koh, L. P., & Ghazoul, J. (2008). Biofuels, biodiversity, and people: understanding the conflicts and finding opportunities. *Biological conservation*, 141(10), 2450-2460.
- Koh, L. P., Miettinen, J., Liew, S. C., & Ghazoul, J. (2011). Remotely sensed evidence of tropical peatland conversion to oil palm. *Proceedings of the National Academy of Sciences*, 108(12), 5127-5132.
- Knudby, A. (2021). *Remote Sensing*. <https://ecampusontario.pressbooks.pub/remotesensing/>.
- Lee, K. A., Gan, W. S., & Kuo, S. M. (2009). *Subband adaptive filtering: theory and implementation*. John Wiley & Sons.
- Lee, J. S. H., Wich, S., Widayati, A., & Koh, L. P. (2016). Detecting industrial oil palm plantations on Landsat images with Google Earth Engine. *Remote Sensing Applications: Society and Environment*, 4, 219-224.
- Li, L., Dong, J., Tenku, S. N., & Xiao, X. (2015). Mapping oil palm plantations in Cameroon using PALSAR 50-m orthorectified mosaic images. *Remote Sensing*, 7(2), 1206-1224.
- Li, M., & Bijker, W. (2019). Vegetable classification in Indonesia using Dynamic Time Warping of Sentinel-1A dual polarization SAR time series. *International Journal of Applied Earth Observation and Geoinformation*, 78, 268-280.
- Lucey, J.M., Barclay, H., Gray, C.L., Luke, S.H., Nainar, A., Turner, E.C., Reynolds, G., Slade, E., Snaddon, J., Struebig, M. and Walsh, R. (2018). Simplified Guide: Management and Rehabilitation of Riparian Reserves. *Kuala Lumpur: RSPO, RSPO Secretariat Sdn Bhd*.
- Luke, S. H., Slade, E. M., Gray, C. L., Annammala, K. V., Drewer, J., Williamson, J., Agama, A., Ationg, M., Mitchell, S., Vairappan, S., & Struebig, M. J. (2019). Riparian buffers in tropical agriculture: Scientific support, effectiveness and directions for policy. *Journal of Applied Ecology*, 56(1), 85-92.
- Ma, L., Liu, Y., Zhang, X., Ye, Y., Yin, G., & Johnson, B. A. (2019). Deep learning in remote sensing applications: A meta-analysis and review. *ISPRS journal of photogrammetry and remote sensing*, 152, 166-177.
- Mandal, D., Vaka, D. S., Bhogapurapu, N. R., Vanama, V. S. K., Kumar, V., Rao, Y. S., & Bhattacharya, A. (2019). Sentinel-1 SLC preprocessing workflow for polarimetric applications: A generic practice for generating dual-pol covariance matrix elements in SNAP S-1 toolbox.
- Maretto, R. V., Fonseca, L. M., Jacobs, N., Körting, T. S., Bendini, H. N., & Parente, L. L. (2021). Spatio-temporal deep learning approach to map deforestation in amazon rainforest. *IEEE Geoscience and Remote Sensing Letters*, 18(5), 771-775.
- McCarthy, J. F., Gillespie, P., & Zen, Z. (2012). Swimming upstream: local Indonesian production networks in “globalized” palm oil production. *World development*, 40(3), 555-569.
- Media Center Riau (2023, June 21). *Pemprov Riau Targetkan RTRW di 12 Kabupaten/Kota Selesai Tahun Ini* [Riau Provincial Government Targets RTRW in 12 Regencies/Cities to be Completed This Year]. Official Riau Province Government Website. <https://www.riau.go.id/home/content/2023/06/21/17090-pemprov-riau-targetkan-rtrw-di-12-kabupatenkota-selesai-tahun>
- Meijaard, E., Garcia-Ulloa, J., Sheil, D., Wich, S. A., Carlson, K. M., Juffe-Bignoli, D., & Brooks, T. M. (2018). Oil palm and biodiversity. *A situation analysis by the IUCN Oil Palm Task Force*.
- Mercer, E. V., Mercer, T. G., & Sayok, A. K. (2014). Effects of forest conversions to oil palm plantations on freshwater macroinvertebrates: a case study from Sarawak, Malaysia. *Journal of Land Use Science*, 9(3), 260-277.
- Miettinen, J., & Liew, S. C. (2011). Separability of insular Southeast Asian woody plantation species in the 50 m resolution ALOS PALSAR mosaic product. *Remote Sensing Letters*, 2(4), 299-307.
- Miettinen, J., Shi, C., & Liew, S. C. (2016). Land cover distribution in the peatlands of Peninsular Malaysia, Sumatra and Borneo in 2015 with changes since 1990. *Global Ecology and Conservation*, 6, 67-78.
- Miettinen, J., Gaveau, D. L., & Liew, S. C. (2018). Comparison of visual and automated oil palm mapping in Borneo. *International Journal of Remote Sensing*, 40(21), 8174-8185.
- Mitchell, S. L., Edwards, D. P., Bernard, H., Coomes, D., Jucker, T., Davies, Z. G., & Struebig, M. J. (2018). Riparian reserves help protect forest bird communities in oil palm dominated landscapes. *Journal of Applied Ecology*, 55(6), 2744-2755.
- Monsalve-Tellez, J. M., Torres-León, J. L., & Garcés-Gómez, Y. A. (2022). Evaluation of SAR and Optical Image Fusion Methods in Oil Palm Crop Cover Classification Using the Random Forest Algorithm. *Agriculture*, 12(7), 955.

- Morel, A. C., Saatchi, S. S., Malhi, Y., Berry, N. J., Banin, L., Burslem, D., Nilus, R., & Ong, R. C. (2011). Estimating aboveground biomass in forest and oil palm plantation in Sabah, Malaysian Borneo using ALOS PALSAR data. *Forest Ecology and Management*, 262(9), 1786-1798
- Mullissa, A. G., Persello, C., & Stein, A. (2019). PolSARNet: A deep fully convolutional network for polarimetric SAR image classification. *IEEE Journal of selected topics in applied earth observations and remote sensing*, 12(12), 5300-5309.
- Murphy, D. J., Goggin, K., & Paterson, R. R. M. (2021). Oil palm in the 2020s and beyond: challenges and solutions. *CABI agriculture and bioscience*, 2(1), 1-22.
- Muzakki, F. (2021). *Detecting of natural to oil palm conversion in tropical wetlands based on sentinel imagery using deep learning* [Unpublished master's thesis]. Faculty of ITC, University of Twente.
- Nomura, K., Mitchard, E. T., Patenaude, G., Bastide, J., Oswald, P., & Nwe, T. (2019). Oil palm concessions in southern Myanmar consist mostly of unconverted forest. *Scientific reports*, 9(1), 1-9.
- Nooni, I. K., Duker, A. A., Van Duren, I., Addae-Wireko, L., & Osei Jnr, E. M. (2014). Support vector machine to map oil palm in a heterogeneous environment. *International journal of remote sensing*, 35(13), 4778-4794.
- Numata, I., Elmore, A. J., Cochrane, M. A., Wang, C., Zhao, J., & Zhang, X. (2022). Deforestation, plantation-related land cover dynamics and oil palm age-structure change during 1990–2020 in Riau Province, Indonesia. *Environmental Research Letters*, 17(9), 094024.
- OECD/FAO (2021), *OECD-FAO Agricultural Outlook 2021-2030*, OECD Publishing, Paris.
- Prince, S. J. D. (2023) *Understanding Deep Learning*. The MIT Press.
- Pohl, C., Kanniah, K. D., & Loong, C. K. (2016, July). Monitoring oil palm plantations in Malaysia. In *2016 IEEE International Geoscience and Remote Sensing Symposium (IGARSS)* (pp. 2556-2559). IEEE.
- Pohl, C., & Van Genderen, J. (2016). *Remote sensing image fusion: A practical guide*. CRC Press.
- Ronneberger, O., Fischer, P., & Brox, T. (2015, October). U-net: Convolutional networks for biomedical image segmentation. In *International Conference on Medical image computing and computer-assisted intervention* (pp. 234-241). Springer, Cham.
- Rukmana, D. (2015). The change and transformation of Indonesian spatial planning after Suharto's new order regime: The case of the Jakarta metropolitan area. *International Planning Studies*, 20(4), 350-370.
- Sarzynski, T., Giam, X., Carrasco, L., & Lee, J. S. H. (2020). Combining radar and optical imagery to map oil palm plantations in Sumatra, Indonesia, using the Google Earth Engine. *Remote Sensing*, 12(7), 1220.
- Sebastianelli, A., Del Rosso, M. P., Mathieu, P. P., & Ullo, S. L. (2021). Paradigm selection for Data Fusion of SAR and Multispectral Sentinel data applied to Land-Cover Classification. *arXiv preprint arXiv:2106.11056*.
- Shaharum, N. S. N., Shafri, H. Z. M., Ghani, W. A. W. A. K., Samsatli, S., Al-Habshi, M. M. A., & Yusuf, B. (2020). Oil palm mapping over Peninsular Malaysia using Google Earth Engine and machine learning algorithms. *Remote Sensing Applications: Society and Environment*, 17, 100287.
- Sheaves, M., Johnston, R., Miller, K., & Nelson, P. N. (2018). Impact of oil palm development on the integrity of riparian vegetation of a tropical coastal landscape. *Agriculture, Ecosystems & Environment*, 262, 1-10.
- Sheil, D., Casson, A., Meijaard, E., Van Noordwijk, M., Gaskell, J., Sunderland-Groves, J., Wertz, K. and Kanninen, M. (2009). *The impacts and opportunities of oil palm in Southeast Asia: What do we know and what do we need to know?* (Vol. 51, pp. 1-19). Bogor, Indonesia: Center for International Forestry Research.
- Shigetomi, Y., Ishimura, Y., & Yamamoto, Y. (2020). Trends in global dependency on the Indonesian palm oil and resultant environmental impacts. *Scientific Reports*, 10(1), 1-11.
- Silalahi, F. T. R., Simatupang, T. M., & Siallagan, M. P. (2020). Biodiesel produced from palm oil in Indonesia: Current status and opportunities. *AIMS Energy*, 8(1), 81-101.
- Solórzano, J. V., Mas, J. F., Gao, Y., & Gallardo-Cruz, J. A. (2021). Land use land cover classification with U-net: Advantages of combining sentinel-1 and sentinel-2 imagery. *Remote Sensing*, 13(18), 3600.
- Torbick, N., Ledoux, L., Salas, W., & Zhao, M. (2016). Regional mapping of plantation extent using multisensor imagery. *Remote Sensing*, 8(3), 236.
- Trisasongko, B. H., Panuju, D. R., Afif, Z., Haptadi, Y., & Shariff, A. R. (2022). Mapping Oil Palm Plantations in the Fringe of Sebangau National Park, Central Kalimantan, Indonesia. *Advances in Remote Sensing for Forest Monitoring*, 167-178.
- Xu, Y., Yu, L., Li, W., Ciais, P., Cheng, Y., & Gong, P. (2020). Annual oil palm plantation maps in Malaysia and Indonesia from 2001 to 2016. *Earth System Science Data*, 12(2), 847-867.
- Yuan, X., Shi, J., & Gu, L. (2021). A review of deep learning methods for semantic segmentation of remote sensing imagery. *Expert Systems with Applications*, 169, 114417.

- Zeng, J., Tan, M.L., Tew, Y.L., Zhang, F., Wang, T., Samat, N., Tangang, F. and Yusop, Z. (2022). Optimization of Open-Access Optical and Radar Satellite Data in Google Earth Engine for Oil Palm Mapping in the Muda River Basin, Malaysia. *Agriculture*, 12(9), 1435.
- Zhu, X.X., Montazeri, S., Ali, M., Hua, Y., Wang, Y., Mou, L., Shi, Y., Xu, F. and Bamler, R. (2021). Deep learning meets SAR: Concepts, models, pitfalls, and perspectives. *IEEE Geoscience and Remote Sensing Magazine*, 9(4), 143-172.

APPENDIX

Appendix 1.

An interactive view of the oil palm map along rivers produced from this study can be accessed at:

<https://bit.ly/oilpalmrivers>